

Supporting Information Anisotropic Quantum Well Electro-Optics in Few-Layer Black Phosphorus

Michelle C. Sherrott^{1,2†}, William S. Whitney^{3†}, Deep Jariwala^{1,2,^}, Souvik Biswas¹, Cora M. Went^{2,3}, Joeson Wong¹, George R. Rossman⁴, Harry A. Atwater^{*1,2,5}

1. Thomas J. Watson Laboratory of Applied Physics, California Institute of Technology, Pasadena, CA 91125, USA
2. Resnick Sustainability Institute, California Institute of Technology, Pasadena, CA 91125, USA
3. Department of Physics, California Institute of Technology, Pasadena, CA 91125, USA
4. Division of Geological and Planetary Sciences, California Institute of Technology, Pasadena, CA 91125, USA
5. Joint Center for Artificial Photosynthesis, California Institute of Technology, Pasadena, CA 91125, USA

† Equal contributors

^ Current affiliation, Department of Electrical and Systems Engineering, University of Pennsylvania, Philadelphia, PA, 19104, USA

*Corresponding author: Harry A. Atwater (haa@caltech.edu)

S1. Identification of Crystal Axes:

To identify the principal crystal axes of the BP flakes, cross-polarization microscopy was used. Incident light passes through a linear polarizer, then the sample, and finally through a second, orthogonal linear polarizer. This technique has been previously described^[1]. By rotating the sample, the fast and slow optical axes (and hence crystal axes) are identified.

S2. AFM Characterization of Flake Thickness:

To characterize the thickness of the BP flakes, AFM measurements are made of the entire device stack. Cross-cuts of AFM images of the flakes are shown in Figure S1. We note that, as previously described, AFM measures a thickness 2 – 3 nm larger than the true value, due to the presence of thin phosphorus oxide layers at each interface^[2]. Moreover, we note that the presence of the top oxide and nickel coatings prevent perfectly accurate determination of thickness, and therefore we additionally determine thickness based on the energy levels of the band gap and intersubband transitions.

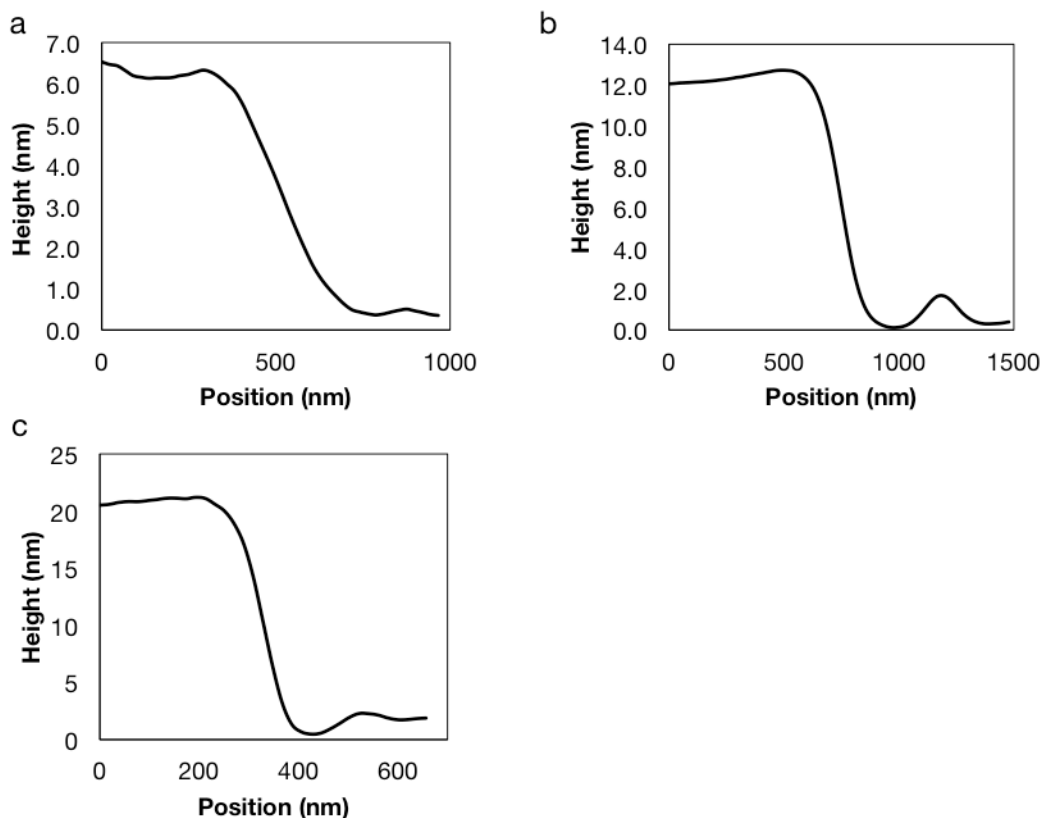


Figure S1 AFM Characterization of Flake Thickness. a) AFM crosscut of '3.5 nm' thick flake, showing measured thickness of 6.5 nm. b) AFM crosscut of '8.5 nm' thick flake, showing measured thickness of 11.5 nm. c) AFM crosscut of '20 nm' thick flake, showing measured thickness of 20 nm. Thicknesses have some uncertainty due to Ni/Al₂O₃ top layers.

S3. Tunability for 8.5 nm Flake along Zigzag Axis:

Fourier transform infrared spectroscopy is used to measure electrical tunability of extinction for light polarized along the zig-zag crystal axis of the 8.5 nm flake, as with the 3.5 nm flake. The corresponding spectra for tunability of the floating device under an applied field and contacted device under direct gating are shown in Fig. S2a and S2b, respectively. No tunability is seen for this polarization, as with the 3.5 nm flake.

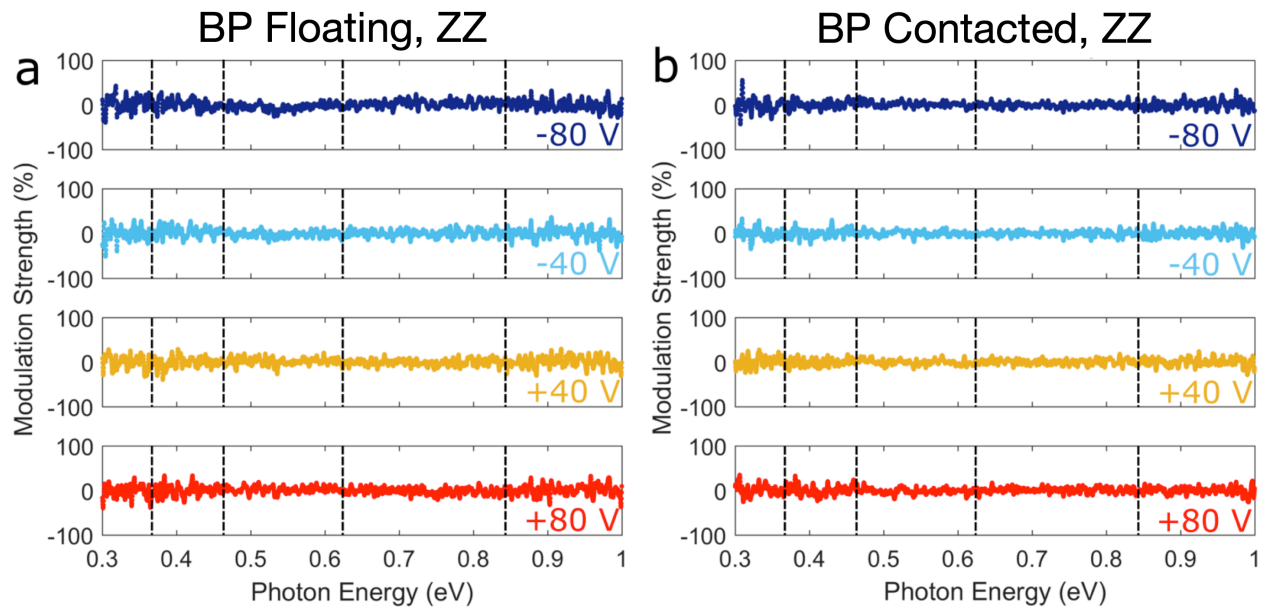


Figure S2. Tunability for 8.5 nm Flake along Zigzag Axis. a) Tunability of BP oscillator strength with field applied to floating device, for light polarized along the ZZ axis. b) Tunability of BP oscillator strength with gating of contacted device, for light polarized along the ZZ axis.

S4. Tunability for 8.5 nm Flake at Lower Energies:

To better understand the behavior of the QCSE at the band edge of the 8.5 nm flake, a second measurement was made of electrical tunability of extinction for light polarized along the armchair crystal axis of the 8.5 nm flake using a KBr beamsplitter instead of CaF_2 . With better resolution at lower photon energies, clear QCSE redshifting of intersubband transitions can be seen at the lowest transition energies. The tunability strength is plotted in arbitrary units, since the extinction tunability is still normalized to the CaF_2 extinction / oscillator strength maximum.

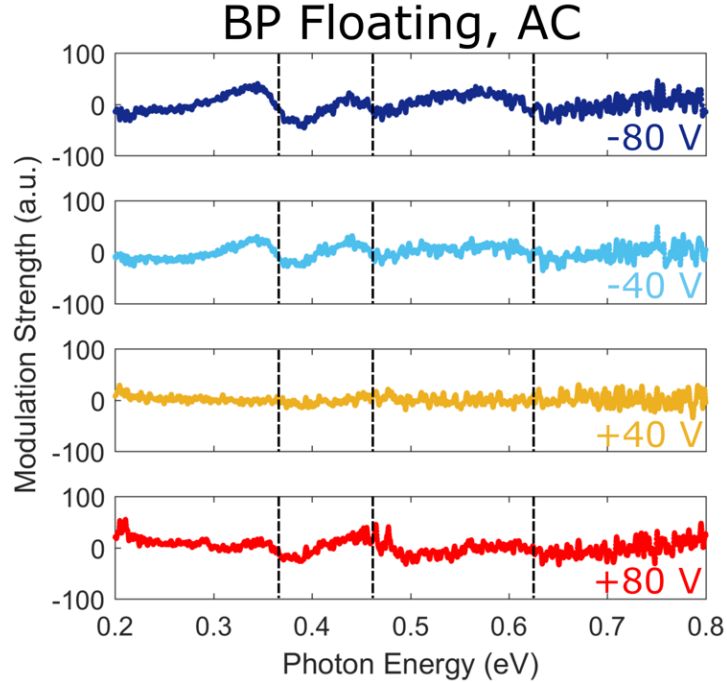


Figure S3. Tunability for 8.5 nm Flake at Lower Energies. Tunability of BP oscillator strength with field applied to floating device, for light polarized along the AC axis, measured at lower photon energies.

S5. Optical Response of Top Contact Material:

In order to verify that no interference effects or spurious absorption features are present in the fabricated device for visible measurements, we performed full wave Finite Difference Time Domain (FDTD) simulations using the Lumerical software package. We verify that the transmittance through 5 nm Ni/90 nm Al_2O_3 /5 nm Ni/0.5 μm SrTiO_3 is featureless, and therefore we can be confident that all tunability is due to the BP. For this reason, we select Ni as the semi-transparent top and bottom-contact and 45 nm thick top and bottom gate dielectrics of Al_2O_3 .

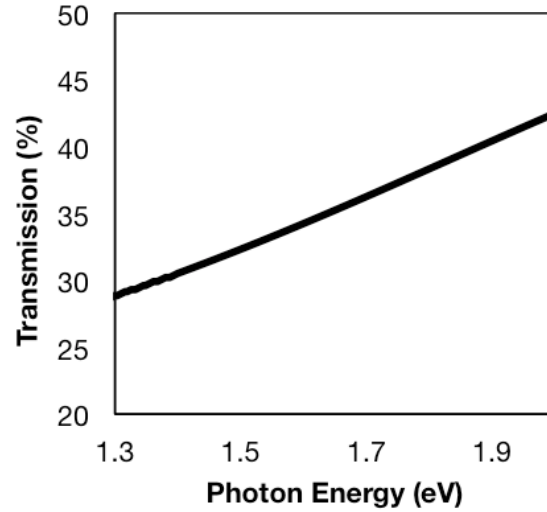


Figure S4. Optical Response of Top Contact Material. FDTD simulation results of transmittance through Ni/Al₂O₃/Ni/SrTiO₃ superstrate/substrate for visible BP measurements. No features are observed.

S6. High reflectance modulation of 6 nm BP flake:

In order to demonstrate that thin BP films can generate technologically compelling absolute modulation depths, we present armchair-axis FTIR reflectance data for a 6 nm flake. This data, for which reflectance at 100 V is normalized to reflectance at zero bias, is presented in Figure S5. The device structure consists of 6 nm BP on 285 nm SiO₂ on Si, with a 10 nm Al₂O₃ cap. Further, the observed modulation depth can be dramatically enhanced by integrating the BP into a resonant optical cavity, as described in Fig. 5 in the main text.

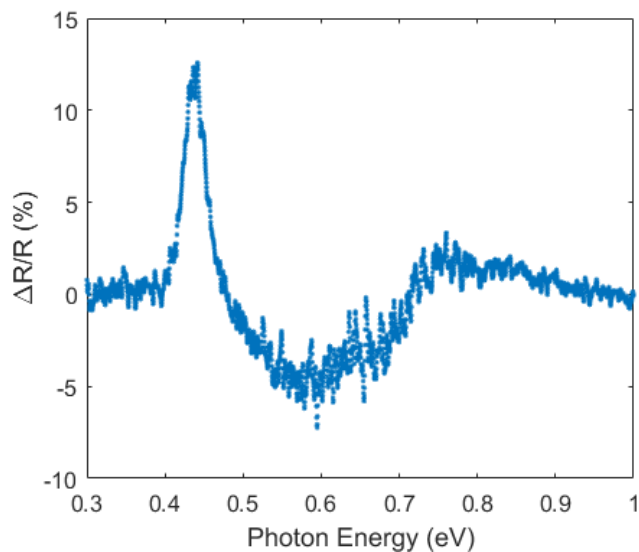


Figure S5. High reflectance modulation of 6 nm BP flake. Armchair-axis FTIR reflectance is shown for 100 V bias, normalized to the zero bias reflectance. Data taken at room temperature under ambient conditions.

S7. Comparison of Extinction Modulation to Theory

We have used theory results for the tunable complex refractive index of black phosphorus to calculate the extinction modulation predicted for a device like those presented in Fig. 2 and Fig. 3, to allow us to compare our results to available theory. This theory work treats the quantum-confined Stark effect and band filling effects for a 5 nm black phosphorus flake using a self-consistent Schrödinger-Poisson model in combination with a Kubo formula to arrive at a charge density dependent optical conductivity.³ We use those reported optical constants and a transfer matrix model to calculate extinction modulation, which we present in Fig. S6 in the same units of modulation strength that we use in the main text. We see a predicted modulation strength and trends that qualitatively match those seen in experiment: redshifting optical transition energies, and the appearance of absorption consistent with a “forbidden” optical transition between conduction and valence subbands with different quantum numbers. More details on the energies of these transitions are available in Lin, et al.³

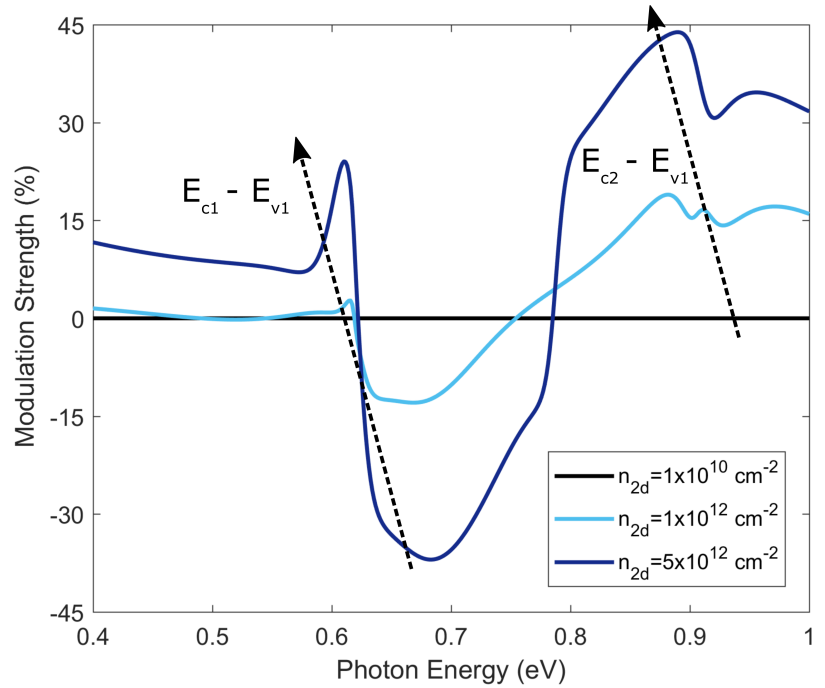


Figure S6. Predicted modulation strength for a device like those in Fig. 2 and Fig. 3, with a 5 nm black phosphorus flake, based on a transfer matrix calculation and theoretical treatment of the electrically tunable complex refractive index of black phosphorus. The predicted modulation strength and trends qualitatively match those seen in experiment.

References:

- (1) Whitney, W. S.; Sherrott, M. C.; Jariwala, D.; Lin, W.-H.; Bechtel, H. A.; Rossman, G. R.; Atwater, H. A. *Nano Letters* **2017**, *17*, 78-84.
- (2) Tian, H.; Guo, Q.; Xie, Y.; Zhao, H.; Li, C.; Cha, J. J.; Xia, F.; Wang, H. *Advanced Materials* **2016**, *28*, 4991-4997.
- (3) Lin, C.; Grassi, R.; Low, T.; Helmy, A. S. *Nano Letters* **2016**, *16*, 1683-1689.